agronomy

Article

Identification of Reactive Oxygen Species Genes Mediating Resistance to *Fusarium verticillioides* in the Peroxisomes of Sugarcane

Xiang Li [1,2,3,†], Yijing Gao [1,2,†], Cuifang Yang [1,2,†], Hairong Huang [1,2], Yijie Li [1,2], Shengfeng Long [1], Hai Yang [1], Lu Liu [1,2], Yaoyang Shen [1] and Zeping Wang [1,*]

[1] Guangxi Academy of Agricultural Sciences, Key Laboratory of Sugarcane Biotechnology and Genetic Improvement (Guangxi), Ministry of Agriculture and Rural Affairs, Guangxi Key Laboratory of Sugarcane Genetic Improvement, Nanning 530007, China; lixiang@gxaas.net (X.L.); gaoyijing@gxaas.net (Y.G.); yangcuifang-713@gxaas.net (C.Y.); hhrong999@gxaas.net (H.H.); liyijie@gxaas.net (Y.L.); longshengfeng@gxaas.net (S.L.); yanghai@gxaas.net (H.Y.); lu.liu@gxaas.net (L.L.); shenyaoyang@gxaas.net (Y.S.)
[2] Guangxi Key Laboratory of Sugarcane Genetic Improvement, Nanning 530007, China
[3] Guangxi Key Laboratory of Quality and Safety Control for Subtropical Fruits, Guangxi Subtropical Crops Research Institute, Nanning 530001, China
* Correspondence: wangzeping@gxaas.net
† These authors contributed equally to this work.

Abstract: Pokkah boeng disease (PBD), which is caused by *Fusarium verticillioides*, is a major sugarcane disease in Southeast Asian countries. Breeding varieties to become resistant to *F. verticillioides* is the most effective approach for minimizing the damage caused by PBD, and identifying genes mediating resistance to PBD via molecular techniques is essential. The production of reactive oxygen species (ROSs) is one of a cell's first responses to pathogenic infections. Plant peroxisomes play roles in several metabolic processes involving ROSs. In this study, seedlings of YT94/128 and GT37 inoculated with *F. verticillioides* were used to identify PBD resistance genes. The cells showed a high degree of morphological variation, and the cell walls became increasingly degraded as the duration of the infection increased. There was significant variation in H_2O_2 accumulation over time. Catalase, superoxide dismutase, and peroxidase activities increased in both seedlings. Analysis of differentially expressed genes (DEGs) revealed that peroxidase-metabolism-related genes are mainly involved in matrix protein import and receptor recycling, adenine nucleotide transport, peroxisome division, ROS metabolism, and processes related to peroxisomal membrane proteins. The expression levels of *SoCATA1* and *SoSOD2A2* gradually decreased after sugarcane infection. *F. verticillioides* inhibited the expressions of C5YVR0 and C5Z4S4. Sugarcane infection by *F. verticillioides* disrupts the balance of intracellular ROSs and increases the cell membrane's lipid peroxidation rate. Defense-related enzymes play a key regulatory role in maintaining a low, healthy level of ROSs. The results of this study enhance our understanding of the mechanism through which peroxisomes mediate the resistance of sugarcane to PBD and provide candidate genes that could be used to breed varieties with improved traits via molecular breeding.

Keywords: sugarcane; resistance; fungal infection; biotic stress; plant–microbe interactions

Citation: Li, X.; Gao, Y.; Yang, C.; Huang, H.; Li, Y.; Long, S.; Yang, H.; Liu, L.; Shen, Y.; Wang, Z. Identification of Reactive Oxygen Species Genes Mediating Resistance to *Fusarium verticillioides* in the Peroxisomes of Sugarcane. *Agronomy* **2024**, *14*, 2640. https://doi.org/10.3390/agronomy14112640

Academic Editor: Junhua Peng

Received: 11 September 2024
Revised: 31 October 2024
Accepted: 5 November 2024
Published: 8 November 2024

1. Introduction

Sugarcane (*Saccharum* spp. interspecific hybrids) is a globally significant source of sugar and biofuel, and it is thus one of the world's most valuable cash crops [1]. However, biotic and abiotic stresses have major effects on sugarcane yields. Diseases, such as pokkah boeng disease (PBD), as well as sugarcane mosaic virus, sugarcane smut, ratoon stunting disease, and sugarcane rust [2], are some of the main biotic stresses negatively affecting sugarcane yields. PBD has a significantly negative effect on sugarcane production and

reduces the quality of its juice, which threatens the safe and sustainable development of the sugar industry in Southeast Asian countries [3], including China [4].

Fusarium moniliforme (*Ascomycotina*) is the major cause of PBD in the sugarcane area of southeast Asia [5]; the invisible stage involves *Fusarium moniliforme* Sheldon, and the sexual stage involves *Gibberella moniliforme* Wineland. Morphological and molecular phylogenetic analyses have confirmed that *Fusarium* species are associated with PBD in China and that *F. verticillioides* is the dominant species infecting sugarcane [6]. PBD results in the crumpling, twisting, and shortening of sugarcane leaves. It also distorts the leaves, and the entire top (growing point) of the plant dies when the infection in the spindle spreads to the stalk [7].

Previous studies have shown that pathogenic infection induces several physiological and biochemical changes in plant cells, including hypersensitive reactions, callose hypertrophy, changes in protective enzymatic activity, rapid accumulation of disease-related proteins, massive accumulation of secondary substances, and alterations in hormone metabolism [8]. The production of reactive oxygen species (ROSs) is one of the first responses of cells following the recognition of pathogens. Plants employ various enzymatic mechanisms during interactions with pathogens to effectively remove ROSs, including mechanisms involving superoxide dismutase (SOD), catalase (CAT), and peroxidase (POD) [9]. In addition, plants use the enzymatic system to defend against excessive ROSs caused by pathogenic invasion [10].

The peroxisome is a highly dynamic and metabolic organelle involved in several metabolic processes, such as lipid metabolism; photorespiration; detoxification; jasmonic acid biosynthesis; the metabolisms of indole-3-butyric acid (IBA), nitrogen, sulfites, and polyamines; and ROS production and removal [11]. ROS accumulation in plant cells causes irreversible damage, which exacerbates membrane degreasing and over-oxidation [12]. The destruction of the structure and function of biofilms significantly degrades downstream cells, which causes chlorophyll and protein degradation and, thus, premature leaf aging [13]. Peroxisomes enhance H_2O_2 detoxification in various parts of the cell following abiotic treatment, which aids the transmission of signals and promotes the introduction of new proteins involved in defense responses [14]. Therefore, peroxisomes can be used to detect intracellular ROS/redox changes. Peroxisomes also induce rapid and specific responses to stress-related factors [15,16].

The major defense mechanisms employed by sugarcane against pathogens involve physiological and biochemical responses and the protection of plant tissues [17]. Research on smut and sugarcane has shown that the glucoside, dihydric phenols, total sugar content, and free amino acids in sugarcane bud scale tissues are associated with disease resistance at the emergence stage [18]. Furthermore, changes in the activities of acidic or neutral invertases and peroxidases phenylalanine ammonia-lyase (PAL) and tyrosine ammonia-lyase (TAL) are associated with resistance under pathogenic inoculation [19]. Another study has suggested that the sugarcane canopy structure is associated with pathogenic resistance [20]. However, the correlations of physiological indices of nitrogen metabolism, such as ribonucleic acid, soluble protein, nitrate nitrogen, ammonium nitrogen, nitrate reductase, glutamine synthetase, and glutamate synthetase, vary with the resistance degree [21].

The mechanism underlying the response of sugarcane to *F. verticillioides* infection involves several complex metabolic processes. Most of the changes observed during the response to the infection affect the stability of the membrane system and the antioxidant enzymatic system. Peroxisomes contain several enzymes involved in various physiological and metabolic processes, such as the acetaldehyde acid cycle, fatty acid oxidation, and ROS regulation in organisms. Peroxisomes also affect fungal pathogenicity [22]. Recently, there have been relevant reports on the important roles of ROSs in sugarcane diseases, such as sugarcane smut, sugarcane mosaic virus, and sugarcane leaf gum disease [23–25], but there have been no relevant reports on the mechanisms of PBD and ROSs. Although resistance genes can be used to analyze the physiological and biochemical mechanisms underlying the response of sugarcane to PBD, many aspects of ROS homeostasis remain unclear. In this

study, we used previously published transcriptome data [26] for YT94/128 (resistant variety, R), GT37 (susceptible variety, S), and *F. verticillioides* spore suspensions to analyze the network of genes involved in the metabolism of peroxisomes and their expression patterns. The aims of this study were to elucidate the molecular mechanism underlying sugarcane's response to PBD, to uncover how ROS genes mediate the sugarcane growth response to pathogenic infection and the corresponding self-repair mechanism, and to continuously analyze the signaling pathway of ROS accumulation and cell death in sugarcane, as well as its relationships with sugarcane growth and disease resistance, to provide design ideas and functional components for molecular breeding for disease resistance.

2. Materials and Methods

2.1. Experimental Materials

Fresh sugarcane (*Saccharum* spp. interspecific hybrids) stems of YT94/128 (resistant genotype, R) and GT37 (sensitive genotype, S) were planted in a greenhouse. Plants with the same growth status were inoculated with *F. verticillioides* (serial number of NCBI: JAKZJQ000000000) after they had 5–6 leaves. A sterile needle was used to microinject conidial isolate suspensions (10^6 conidia mL^{-1}, 100 μL) into each sugarcane stalk. The plants were shaded and moisturized after inoculation. The greenhouse temperature and humidity were maintained at 20–35 °C and 80.00–85.00%, respectively. Symptoms were observed on the inoculated leaves at 24 h post inoculation (PI) for up to 21 days. Samples with the highest disease index (DSI) were taken from the +1 sugarcane leaf at 14 d PI. Mock inoculation with distilled water was used as the control (CK). The samples were ground in liquid nitrogen and maintained at −80 °C.

2.2. Transmission Electron Microscopy Analysis

Sample fixation: Low volumes ($\leq$1 mm^3) of fresh leaf tissues were used to minimize the mechanical damage caused by pulling, bruising, and squeezing. The tissues were quickly fixed using an electron microscope fixative, dried using a vacuum pump, and then maintained at room temperature (20–25 °C) for 2 h. The tissues were transferred to an approximately 4 °C refrigerator and then rinsed three times using phosphate-buffered saline solution (PBS, pH 7.4) for 15 min each.

Post fixation: The samples were fixed with 1% osmium acid and 0.1 M PBS (pH 7.4) at room temperature (20–25 °C) for 5 h before being rinsed three times with PBS (pH 7.4) for 15 min each time.

Dehydration: The tissues were initially dehydrated using the following alcohol gradient: 30%-50%-70%-80%-90%-95%-100%-100% for 1 h each, and then thoroughly dehydrated with the following gradient: anhydrous ethanol:acetone = 3:1 for 0.5 h, anhydrous ethanol:acetone = 1:1 for 0.5 h, anhydrous ethanol:acetone = 1:3 for 0.5 h, and acetone for 1 h.

Percolation: The samples were treated via the use of 812 embedding medium at different concentrations and times: (1) Acetone:812 embedding medium = 1:1 for 2–4 h then overnight percolation; (2) acetone:812 embedding medium = 1:3 for 2–4 h; (3) pure 812 embedding medium for 5–8 h. The pure 812 embedding medium was added to the embedding plate, and the samples were maintained at 37 °C overnight.

Embedding: The samples were subjected to oven polymerization at 60 °C for 48 h. The sugarcane tissue was sliced into 60–80 nm thick samples using an ultramicrotome.

Staining: Uranium–lead double staining (2% uranium-acetate-saturated alcohol solution and lead citrate; each stain was applied for 15 min) was used to stain the samples. The slices were then dried at room temperature overnight.

2.3. Antioxidant Enzymatic Activity Determination

The nitroblue tetrazolium (NBT) photochemical reduction method was used to determine the SOD activity; the H_2O_2 decomposition method was used to determine the CAT activity, and the guaiacol method was used to determine the POD activity. A Spectra

Max M2 multifunctional spectrometer was used to measure OD values. Histochemical staining methods with diaminobezidine (DAB) were used to examine H_2O_2 accumulation. The content of the H_2O_2 was determined using detection kits, as per the manufacturer's instructions (Suzhou Comin Biotechnology).

2.4. Validation of Relative mRNA Expressions

A quantitative reverse transcription polymerase chain reaction (qRT–PCR) assay was used to quantify 16 relative mRNA expressions selected based on correlational analysis of data on transcriptomes and proteomes involved in peroxisome metabolism [21,26]. Samples were used for RNA extraction with the RNAprep Pure Plant Kit (polysaccharide and polyphenol rich) (Tiangen, Beijing, China). First-strand cDNA was synthesized according to the instructions of the TaKaRa PrimeScript RT reagent kit (Perfect for Real Time) (TaKaRa Biotechnology, Dalian, China). PCR was performed on an ABI 7500 real-time PCR machine (Applied Biosystems, Foster City, CA, USA). The cycling conditions were 10 min at 95 °C, followed by 35 cycles at 94 °C for 15 s and at 60 °C for 60 s. SYBR Green PCR Master Mix (Bio-Rad, Mountain View, CA, USA) was used for qRT-PCR analysis; three biological replicates were performed for each gene, and two technical replicates of each experiment were performed. Target-specific primers were designed from RNA-seq sequences using the NCBI primer designer tool. Relative gene expression levels were calculated using the $2^{-\Delta\Delta CT}$ method [27]. The primers used in this study are listed in Supplementary Table S1, with ACT1 (actin) as the reference gene.

2.5. Western Blotting

Human epidermal keratinocytes (HEKs) and human epidermal melanocytes (HEMs) were incubated under the indicated conditions specified by the supplier and lysed. The total protein was extracted from the leaf tissue specimens and primary cells using RIPA buffer. This was followed by separation using 10% SDS-PAGE and electro-transfer onto a polyvinylidene difluoride membrane (Millipore, Billerica, MA, USA). Non-specific antibody binding was blocked by incubating the membrane in Tris-buffered saline with 0.1% Tween-20 and 5% non-fat dried milk at room temperature for 2 h. The membranes were then incubated with primary antibodies (anti-β-actin (29058-1hz-5/C5 and 30443-1hz-10/C9)) at 4 °C overnight. The membranes were incubated using sugarcane peroxidase (HRP)-conjugated secondary antibody at room temperature for 1 h. An enhanced chemiluminescence substrate (Pierce, Rockford, IL, USA) was used to detect immunoreactive bands, and an LAS-3000 luminescence image analyzer (Fujifilm, Tokyo, Japan) was used for visualization.

2.6. Data Processing and Statistical Analysis

A one-way ANOVA [28] with Dunnett's multiple comparison test [29] was used to analyze antioxidant enzymatic activities. A p-value of < 0.05 was considered as significant, and $p < 0.01$ was considered as highly significant. Excel 2007 software was used to make graphs, and SPSS 22.0 software was used to conduct statistical analyses.

3. Results

3.1. Symptoms and Cytological Changes in Sugarcane

Typical symptoms of *F. verticillioides* infection were observed on the leaves of the sensitive genotype following infection with *F. verticillioides* for different periods; no symptoms were observed on leaves of the resistant genotype. After infection, the apical growing point of S was slightly etiolated, and the base of young leaves was chlorotic. Slightly yellow and irregular reddish specks or stripes were observed (1–7 d PI) (Figure 1A). The infection at the growing point spread up into the stalk, and dark reddish streaks appeared in several internodes (7–14 d PI). The growth of the infected tissues was significantly affected by disease progression compared with that of healthy tissues (14–21 d PI). A transmission electron microscope was used to visualize the infected sugarcane leaf cells (Figure 1B). There

were no nuclei in the sugarcane leaf cells; most cells shrank and were irregular in shape. The cell wall thickness was uneven, and the cell wall was partially destroyed; protoplasts and organelles of the cytoplasm disappeared, and vacuolation of the cytoplasm occurred. Circular residues formed (indicated by the arrows in Figure 1). Fungi were distributed in various areas of the cell. However, S leaves infected with *F. verticillioides* had damaged and degraded organelles. The cell wall was also thin and damaged (Figure 1C). The heart leaf cells were relatively young; nuclei were light colored and had obvious nucleoli. A complete cell membrane was present; the full protoplasts lacked a separated plasmic wall and had a complete cell wall, obvious plasmodesmata, and pronounced swelling and vacuolization of intracellular organelles (Figure 1D). The mitochondria showed moderate and severe swelling; most of the mitochondrial cristae disappeared, and a large number of vacuoles were observed. Vacuoles were not obvious (they might be immature cells that have not developed vacuoles); the cytoplasm was flocculent, and a white crystal was present in the cytoplasm (Figure 1E).

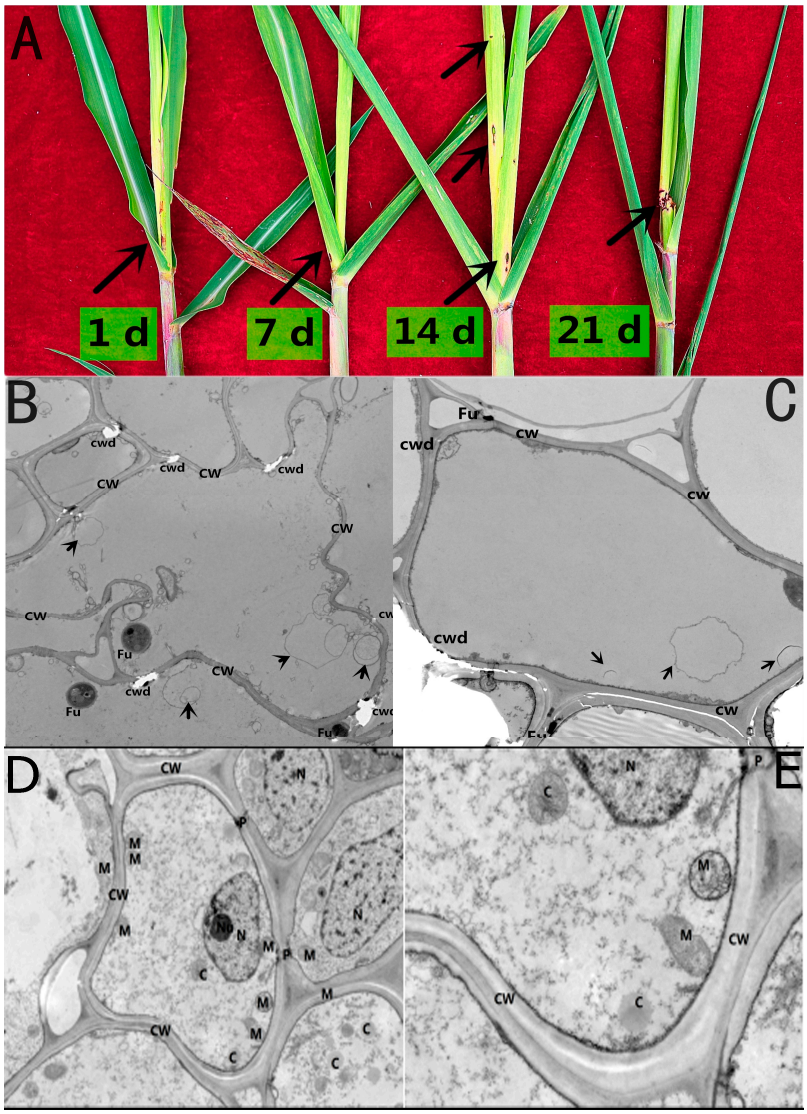

Figure 1. Symptoms and cytological changes in infected sugarcane. (**A**) The common symptoms of infected sugarcane leaves at 1–21 d post inoculation (PI); (**B**,**C**) cytological changes in sugarcane leaves infected with *F. verticillioides*. CW, cell wall; cwd, destroyed cell wall; Fu, fungus; arrows (→) indicate circular residues; (**D**,**E**) cytological changes in non-inoculated sugarcane leaves. M, mitochondria; P, plasmodesmata; C, crystal.

3.2. Accumulation of Key Oxidases in Sugarcane Following F. verticillioides Infection

ROSs have a major effect on the success of pathogenic infection. H_2O_2 accumulates following *F. verticillioides* infection. H_2O_2 accumulation was the highest in S-PI (the sensitive genotype post inoculation), followed by S-CK (the sensitive genotype with a mock inoculation), R-PI (the resistant genotype post inoculation), and R-CK (the resistant genotype with a mock inoculation). H_2O_2 accumulation in each period significantly differed following the inoculation of S. However, no significant differences between R and the other treatments were observed (Figure 2A). The antioxidant enzymes that scavenge H_2O_2 were detected. (i) POD activity rapidly and significantly increased after infection, and this was followed by the steady accumulation of POD. The expression of R was slightly higher than that of S in the same treatment (Figure 2B). (ii) SOD activity significantly increased in both R and S. However, a peak in each curve was observed at 7 d PI for *F. verticillioides*-infected sugarcane, and decreases were observed at subsequent stages. SOD activity was higher in R than in S at every stage, and the difference in each period was significant (Figure 2C). (iii) CAT activity increased in S; a substantial increase was observed at 7–14 d PI, and a rapid increase was observed at 21 d PI. However, no significant differences were observed in R (Figure 2D).

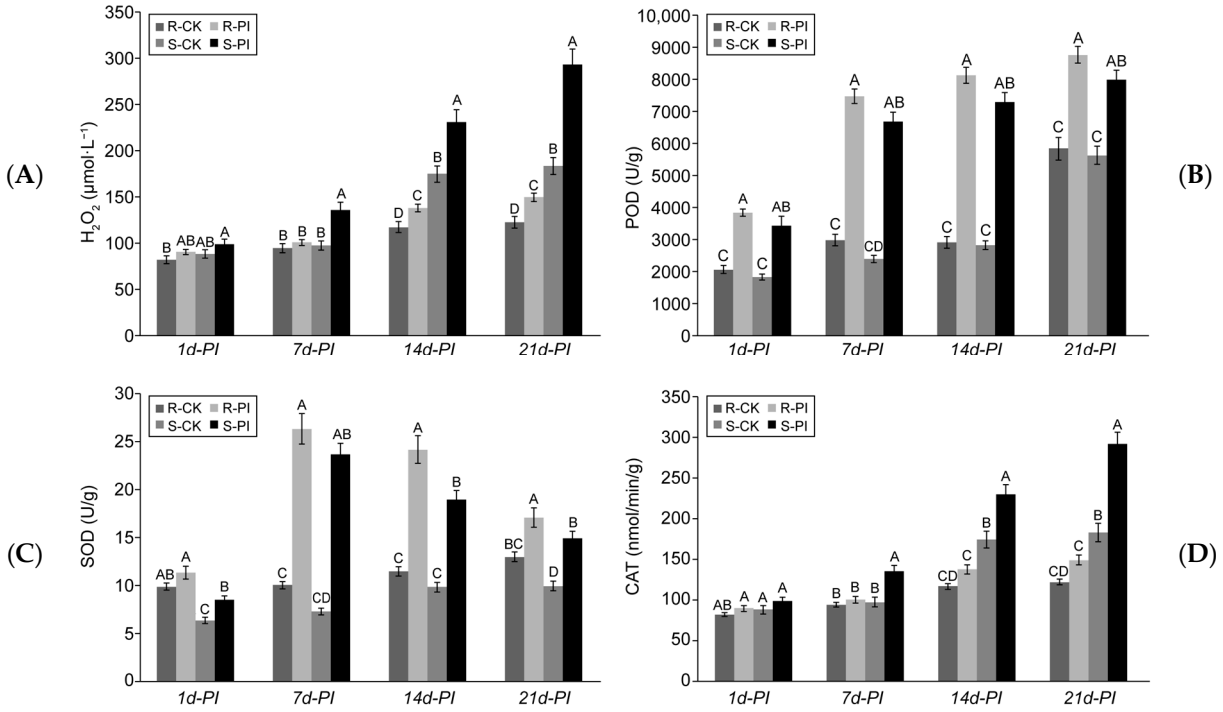

Figure 2. Physiological parameters associated with ROS accumulation. (**A**) H_2O_2, (**B**) POD, (**C**) SOD, and (**D**) CAT. Values indicate the mean fold changes in pathogen-infected sugarcane from 1 to 21 d PI. Error bars represent the standard deviation. Each treatment had three independent biological replicates. The capital letters (A, AB, B, C, BC, D, and CD) above the SD bars indicate significant differences of various physiological indicators at $p < 0.01$ based on Tukey's test. All the average values within each group were arranged from the highest to the lowest. The letter A indicates the maximum value. Afterward, the second value was compared to the maximum value, with the letter B being marked if the difference was significant and the letter A being marked if it was not. Repeated comparisons were based on the value marked with a different letter, compared to the adjacent higher value, and the same letter continues to be marked with no significant difference until the lowest average is marked with a new letter. The same letters mean insignificant differences, and the difference between the two values was significant only if all the letters were different. R-CK, R-PI, S-CK, and S-PI indicate the mock-inoculated YT94/128, pathogen-inoculated YT94/128, mock-inoculated GT37, and pathogen-inoculated GT37, respectively.

3.3. Expressions of Peroxisome Biosynthesis Genes

Peroxisomes enhance H_2O_2 detoxification in various cell parts, transmit signals, and promote the production of new defense-related proteins [30]. Analysis of transcriptome data derived from our previous study [26] and gene annotations (Table 1) of the peroxidase-metabolism-related genes indicated that the sugarcane's response to *F. verticillioides* infection mainly involves matrix protein import, receptor recycling, adenine nucleotide transport, peroxisome division, ROS metabolism, and peroxisomal membrane proteins, including PEX1, PEX2, PEX3, PEX5, PEX6, PEX7, PEX10, PEX12, PEX13, PEX14, PEX16, PEX19, PMP34, PMP70, PXMP2, and MPV17 (Figure 3).

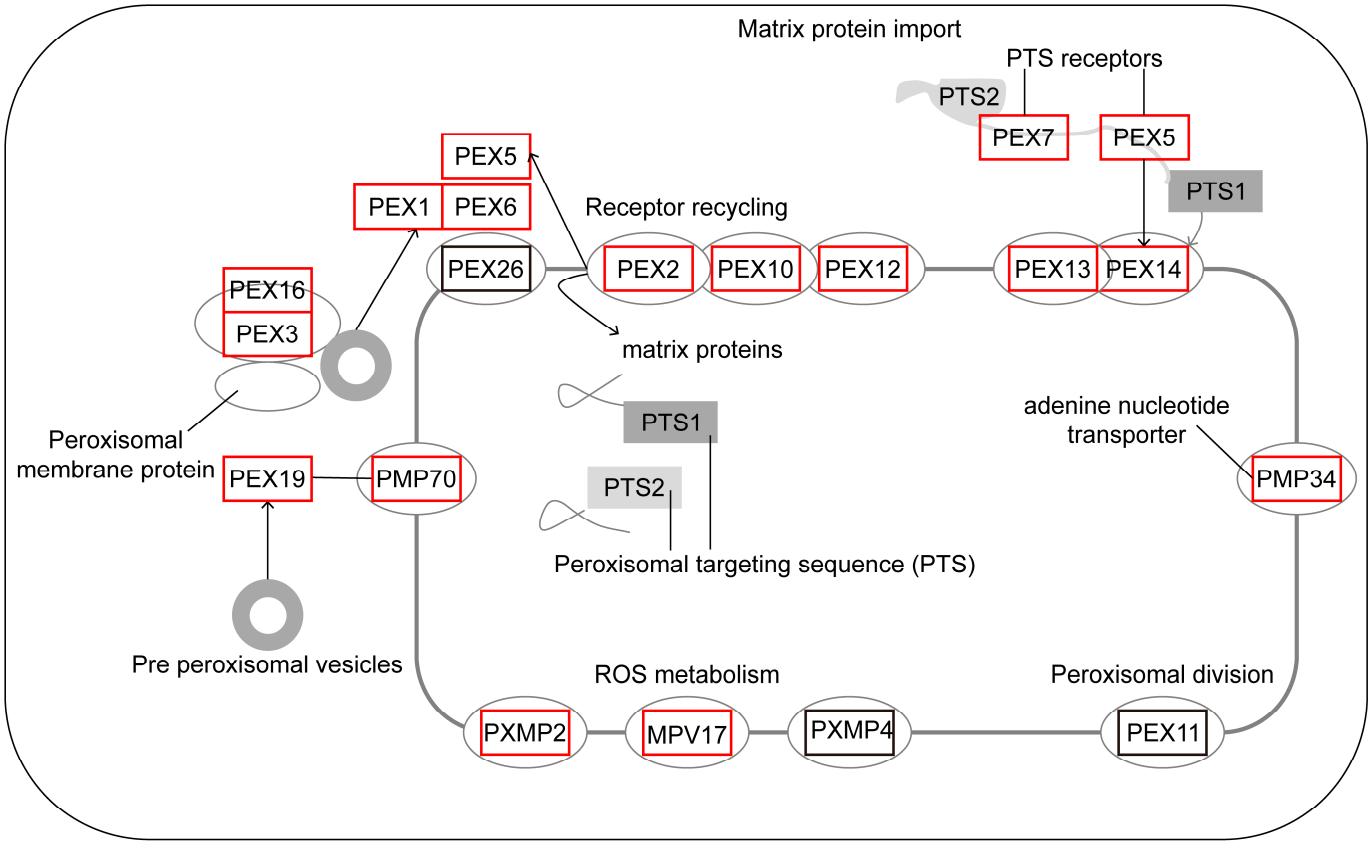

Figure 3. Metabolic pathway of peroxisome-related genes in *F. verticillioides*-infected sugarcane.

During peroxisome biogenesis, all the genes except *PEX6* were increasingly expressed in R following infection (R-PI). *PEX5*, *PEX13*, *PEX14*, and *PMP70* were the most highly expressed genes (Table 1). However, no significant differences in gene expression were observed between R and S following inoculation (R-PI and S-PI). *PMP34* and *MPV17* expressions were significantly lower in R-CK than in S-CK under normal growth, but the expressions of these genes were significantly up-regulated after infection.

Table 1. Data for all the detected peroxisome biosynthesis genes in *F. verticillioides*-infected sugarcane. (Greener and redder colors indicate lower and higher gene expression abundances, respectively).

Metabolic Process	Gene ID	KEGG	Code Protein	Function	R-CK			R-PI			S-CK			S-PI			Significance	
					RPKM [a]	CV [b]	SE [c]	RPKM	CV	SE	RPKM	CV	SE	RPKM	CV	SE	R-PI/R-CK	S-PI/S-CK
Peroxisome biogenesis	*Unigene0033806*	K13341	PEX7	peroxisome biogenesis protein 7	7.9662	0.0697	0.3207	8.8019	0.0146	0.0084	8.6725	0.0310	0.0179	7.1804	0.1271	0.0734	NO	NO
	Unigene0063263	K13342	PEX5	peroxisome biogenesis protein 5-like	44.2071	0.0112	0.2857	50.3211	0.0088	0.0051	48.4445	0.0211	0.0122	50.5650	0.0288	0.0166	NO	NO
	Unigene0051250	K13343	PEX14	LOC100283640 isoform X11	59.2501	0.0210	0.7171	66.8849	0.0094	0.0055	54.5609	0.0061	0.0035	54.8432	0.0355	0.0205	NO	NO
	Unigene0007964	K13344	PEX13	peroxisomal membrane protein 13 isoform X2	70.7417	0.0332	1.3564	84.3885	0.0183	0.0106	82.8340	0.0508	0.0294	117.7248	0.0555	0.0321	NO	NO
	Unigene0057386	K13345	PEX12	peroxisome biogenesis protein 12	1.0384	0.1644	0.0986	1.3756	0.0601	0.0347	1.4643	0.1880	0.1086	1.0259	0.2383	0.1376	NO	NO
	Unigene0003622	K13346	PEX10	LOC100274236 isoform X1	7.5197	0.0602	0.2612	8.4905	0.0600	0.0346	7.7226	0.0804	0.0464	6.7297	0.0629	0.0363	NO	NO
	Unigene0050655	K06664	PEX2	peroxisome biogenesis protein 2-like	0.6116	0.2469	0.0872	0.7423	0.7562	0.4366	1.2340	0.1645	0.0950	0.7335	0.1024	0.0591	NO	NO
	Unigene0053439	K13339	PEX6	peroxisome biogenesis protein 6	11.6791	0.0249	0.1678	11.3455	0.0083	0.0048	12.5484	0.0468	0.0270	10.5095	0.0289	0.0167	NO	NO
	Unigene0069315	K13338	PEX1	peroxisome biogenesis protein 1 isoform X1	7.3921	0.0919	0.3923	8.6209	0.0116	0.0067	7.6606	0.0741	0.0428	6.6528	0.0443	0.0256	NO	NO
	Unigene0004130	K13336	PEX3	lysine and histidine specific transporter	16.5820	0.0415	0.3975	19.9717	0.0775	0.0447	6.6793	0.0285	0.0165	7.6846	0.0935	0.0540	NO	NO
	Unigene0062306	K13335	PEX16	peroxisome biogenesis protein 16 isoform X1	10.4384	0.0446	0.2689	12.8050	0.0359	0.0207	5.3889	0.1053	0.0608	5.8376	0.0508	0.0293	NO	NO
	Unigene0064371	K13337	PEX19	aspartic-type endopeptidase/ pepsin A	14.4008	0.0083	0.0686	23.2056	0.0253	0.0146	9.5224	0.1544	0.0892	16.7123	0.0824	0.0476	YES	YES
	Unigene0067682	K05677	PMP70	Os01g0966100, partial	29.3037	0.0761	1.2867	40.2446	0.0031	0.0018	30.5205	0.0387	0.0223	34.2896	0.0312	0.0180	YES	NO
	Unigene0055607	K13347	PXMP2	peroxisomal membrane protein	6.3976	0.0775	0.2861	7.0398	0.0206	0.0119	6.9736	0.0346	0.0200	5.9972	0.0908	0.0524	NO	NO
	Unigene0074780	K13354	PMP34	peroxisomal adenine nucleotide carrier 1	0.0010	-	-	0.4985	0.4571	0.2639	0.8365	1.4142	0.8165	7.6053	0.1482	0.0856	YES	YES
	Unigene0075468	K13348	MPV17	___	0.0010	-	-	0.6891	0.4085	0.2359	0.0718	1.4142	0.8165	0.3957	0.7074	0.4084	YES	YES

Table 1. *Cont.*

Metabolic Process	Gene ID	KEGG	Code Protein	Function	R-CK			R-PI			S-CK			S-PI			Significance	
					RPKM [a]	CV [b]	SE [c]	RPKM	CV	SE	RPKM	CV	SE	RPKM	CV	SE	R-PI/R-CK	S-PI/S-CK
Antioxidant system	*Unigene0075430*	K03781	CAT	proteasome subunit alpha type-6	0.0010	-	-	0.6608	0.6385	0.3687	0.0010	-	-	0.6853	0.2730	0.1576	YES	YES
	Unigene0072216			CAT	0.0348	1.4142	0.0284	1.0953	0.3181	0.1837	0.1198	1.4142	0.8165	1.1568	0.2896	0.1672	YES	YES
	Unigene0072215			CAT	0.0010	-	-	1.2638	0.4371	0.2523	0.2535	1.4142	0.8165	1.3211	0.3759	0.2170	YES	YES
	Unigene0051330			CAT	29.3319	0.0238	0.4037	48.2154	0.0154	0.0089	25.0659	0.0606	0.0350	34.8034	0.0381	0.0220	YES	YES
	Unigene0039369			CAT-1	186.0828	0.0573	6.1565	101.7058	0.0557	0.0322	226.0953	0.0504	0.0291	147.1190	0.0747	0.0432	YES	YES
	Unigene0038299			CAT	60.9404	0.1336	4.6989	130.1449	0.2192	0.1265	54.2589	0.2117	0.1222	153.2739	0.0772	0.0446	YES	YES
	Unigene0037020			zinc ion binding protein	1.0075	0.1362	0.0792	1.2050	0.0526	0.0304	2.8569	0.1161	0.0671	3.2169	0.0155	0.0090	NO	NO
	Unigene0006408			TPA: CAT 2	7.6359	0.0598	0.2636	5.4813	0.0706	0.0407	24.6224	0.0783	0.0452	19.6959	0.0156	0.0090	NO	YES
	Unigene0073932	k04565	SOD1	Cu/Zn-SOD	0.0010	-	-	5.6634	0.3144	0.1815	0.2573	1.4142	0.8165	3.2312	0.1882	0.1087	YES	YES
	Unigene0053392			SOD 9	4.0918	0.1621	0.3829	3.2999	0.1690	0.0976	6.3614	0.1917	0.1107	6.2701	0.1587	0.0916	NO	NO
	Unigene0051686			Cu/Zn-SOD 2 isoform X3	7.2757	0.0648	0.2723	7.7570	0.2255	0.1302	6.5861	0.1267	0.0731	10.4463	0.1752	0.1011	NO	YES
	Unigene0051680			Cu/Zn-SOD 2 isoform X2	9.3292	0.0429	0.2309	9.8792	0.0863	0.0498	8.3408	0.0380	0.0220	10.0856	0.0441	0.0255	NO	NO
	Unigene0041388			Ring finger protein 3-like	0.3712	0.2642	0.0566	0.2444	1.4142	0.8165	0.0821	0.7071	0.4083	0.0010	-	-	NO	YES
	Unigene0033801			SOD 1a	275.1232	0.0380	6.0387	200.8140	0.0331	0.0191	162.0119	0.0626	0.0361	176.7839	0.0640	0.0369	YES	YES
	Unigene0015729			Cu/Zn-SOD 2-like	9.7619	0.0607	0.3423	9.4188	0.0587	0.0339	7.0985	0.0578	0.0334	7.4083	0.0492	0.0284	NO	NO
	Unigene0076134	k04564	SOD2	Mn-SOD	0.0198	1.4142	0.0162	2.2697	0.8307	0.4796	0.1556	1.4142	0.8165	0.8202	0.3658	0.2112	YES	YES
	Unigene0073241			SOD	0.0010	-	-	0.8986	0.1926	0.1112	0.0374	1.4142	0.8165	0.6176	0.3720	0.2148	YES	YES
	Unigene0059824			SOD precursor	36.1071	0.0310	0.5574	18.5760	0.0043	0.0025	31.9689	0.0606	0.0350	15.2202	0.0357	0.0206	YES	YES
	Unigene0050341			SOD, chloroplast	21.6923	0.0460	0.5765	14.6023	0.0627	0.0362	25.6472	0.0362	0.0209	17.1011	0.0811	0.0468	YES	YES
	Unigene0033124			SOD	80.6034	0.0366	1.7029	81.9991	0.0161	0.0093	62.9326	0.0029	0.0017	67.2948	0.0106	0.0061	NO	NO
	Unigene0074176	k11187	PRDX5	redoxin domain protein	0.0010	-	-	1.6403	0.3757	0.2169	0.0300	1.4142	0.8165	0.7234	0.0963	0.0556	YES	YES
Fatty acid oxidation	*Unigene0049557*	K12261	HPCL2	2-hydroxyphytanoyl-CoA lyase	10.7552	0.0808	0.5015	13.9140	0.0218	0.0126	12.7508	0.1095	0.0632	15.6975	0.0392	0.0226	NO	NO
	Unigene0039674	K00477	PHYH	phytanoyl-CoA dioxygenase 1-like	14.1838	0.0442	0.3620	31.9888	0.0170	0.0098	14.6421	0.0862	0.0498	24.3260	0.0554	0.0320	YES	YES
	Unigene0059982	K00232	ACOX	acyl-coenzyme A oxidase	16.9339	0.0172	0.1683	27.1372	0.0409	0.0236	18.1096	0.0503	0.0291	21.3300	0.0615	0.0355	YES	NO
	Unigene0073157	K07513	ACAA1	3-ketoacyl-CoA thiolase 2, peroxisomal-like	0.0010	-	-	1.4563	0.5443	0.3142	0.1057	1.4142	0.8165	0.9680	0.3247	0.1875	YES	YES
	Unigene0034895	K13237	PDCR	peroxisomal 2,4-dienoyl-CoA reductase	10.6589	0.0553	0.3403	14.5500	0.1055	0.0609	12.6575	0.0617	0.0356	13.1610	0.1843	0.1064	NO	NO

Table 1. *Cont.*

Metabolic Process	Gene ID	KEGG	Code Protein	Function	R-CK			R-PI			S-CK			S-PI			Significance	
					RPKM [a]	CV [b]	SE [c]	RPKM	CV	SE	RPKM	CV	SE	RPKM	CV	SE	R-PI/R-CK	S-PI/S-CK
	Unigene0067682	K05677	ABCD	Os01g0966100, partial	29.3037	0.0761	1.2867	40.2446	0.0031	0.0018	30.5205	0.0387	0.0223	34.2896	0.0312	0.0180	YES	NO
	Unigene0037471	K12633	ECH	δ(3,5)-δ iimport(2,4)-dienoyl-CoA isomerase	0.3408	0.5574	0.1097	0.3579	0.6247	0.3607	0.5305	0.2143	0.1237	0.4221	0.0980	0.0566	NO	NO
	Unigene0072308	K01897	ACSL	BnaA10g20090D	0.7402	-	-	1.6447	0.7731	0.4464	0.0010	1.4142	0.8165	0.1130	0.2041	0.1179	YES	YES
	Unigene0049878	K03426	NUDT12	hydrolase, NUDIX family protein	27.0357	0.0198	0.3089	27.4400	0.0395	0.0228	19.3755	0.0447	0.0258	22.4392	0.0344	0.0199	NO	NO
	Unigene0010648	K01578	MLYCD	malonyl-CoA decarbox	2.7265	0.1003	0.1579	3.7668	0.0921	0.0532	2.8768	0.0639	0.0369	2.6193	0.0335	0.0193	NO	NO

RPKM [a], Reads per kilobase of transcript per million mapped reads, and the source data derived from our previous study [26]. [b] CV, coefficient of variation. [c] SE, Standard Error.

The sugarcane antioxidant system genes included eight *CAT* genes, twelve *SOD* genes, and one *PRDX5* gene (Table 1). *CAT* genes, such as *Unigene0075430*, *Unigene0072216*, *Unigene0072215*, *Unigene0038299*, and *Unigene0037020*, were more highly expressed in S than in R after inoculation. However, most of the genes were barely expressed following the mock inoculation. For example, *Unigene0039369* and *Unigene0038299* were significantly expressed, but their expressions substantially changed after infection. The expressions of *SOD1* genes, including *Unigene0073932*, *Unigene0051686*, *Unigene0051680*, and *Unigene0041388*, were consistently up-regulated or down-regulated apparently in R and S after *F. verticillioides* infection. By contrast, *Unigene0033801* and *Unigene0015729* exhibited the opposite expression patterns. The expressions of four *SOD2* genes, including *Unigene0076134*, *Unigene0073241*, *Unigene0059824*, and *Unigene0050341*, were consistently up-regulated or down-regulated obviously in R and S. The expression of *PRDX5* (*Unigene0074176*) was significantly low during normal sugarcane growth, but its expression significantly increased after infection.

Peroxisomes are an essential organelle for fatty acid oxidation. We identified two α-oxidized fatty acid genes (*Unigene0049557* and *Unigene0039674*), two β-oxidized fatty acid genes (*Unigene0059982* and *Unigene0073157*), four unsaturated β-oxidized fatty acid genes (*Unigene0034895*, *Unigene0067682*, *Unigene0037471,* and *Unigene0072308*), and two oxidized fatty acid genes (*Unigene0049878* and *Unigene0010648*) (Table 1). The expressions of most genes (except for *Unigene0072308* and *Unigene0049878*) were slightly lower in R-CK or the same as in S-CK under natural growth conditions. However, the expressions of most genes (except for *Unigene0037471* and *Unigene0010648*) increased after pathogenic infection.

3.4. Identification of Genes in Sugarcane

qRT-PCR was used to verify the expression patterns of the 16 genes selected for peroxisome biosynthesis (Table 1). The expressions of *Unigene0039369* and *Unigene0059824* gradually decreased after infection, and, conversely, the expressions of the left 13 genes increased with increasing degree of pathogenic infection and were significantly higher in the late infection period compared with the mock inoculation and early infection period (Figure 4). The expression of *Unigene0038299* increased the most, with 25-fold and 20-fold increases in R-PI and S-PI, respectively. The expressions of *Unigene0039369* and *Unigene0059824* were decreased by 2 and 1.8 times, respectively, and there was no significant difference between the amounts of reductions in R-PI and S-PI. With the exception of *Unigene0007964*, the expression levels of 15 genes were significantly higher in R-PI than in S-PI.

3.5. Protein Extraction and Expression

Gene Ontology and Kyoto Encyclopedia of Genes and Genomes analyses (Figure 5) revealed that C5YVR0 belonged to the iron/manganese superoxide dismutase family, which plays a role in catalyzing the superoxide dismutase redox reaction ($2\ H^+ + 2$ superoxide = $H_2O_2 + O_2$). C5YVR0 destroys radicals that are toxic to biological systems. C5Z4S4 is an acyl-coenzyme A oxidase 2 that catalyzes the peroxisomal reaction (acyl-CoA + O_2 = *trans*-2,3-dehydroacyl-CoA + hydrogen peroxide). C5Z4S4 plays key roles in fatty acid β-oxidation, lipid homeostasis, and long-chain fatty acid metabolic processes. The WB antibody was identified, and their encoded proteins were identified to verify the functions of *SOCATA1* and *SOSOD2A2*. C5YVR0 and C5Z4S4 had a specific band at approximately 25 kDa (Figure 6), and their expression levels were the highest in R-PI, followed by R-CK, S-PI, S-CK, R-PI, S-PI, R-CK, and S-CK.

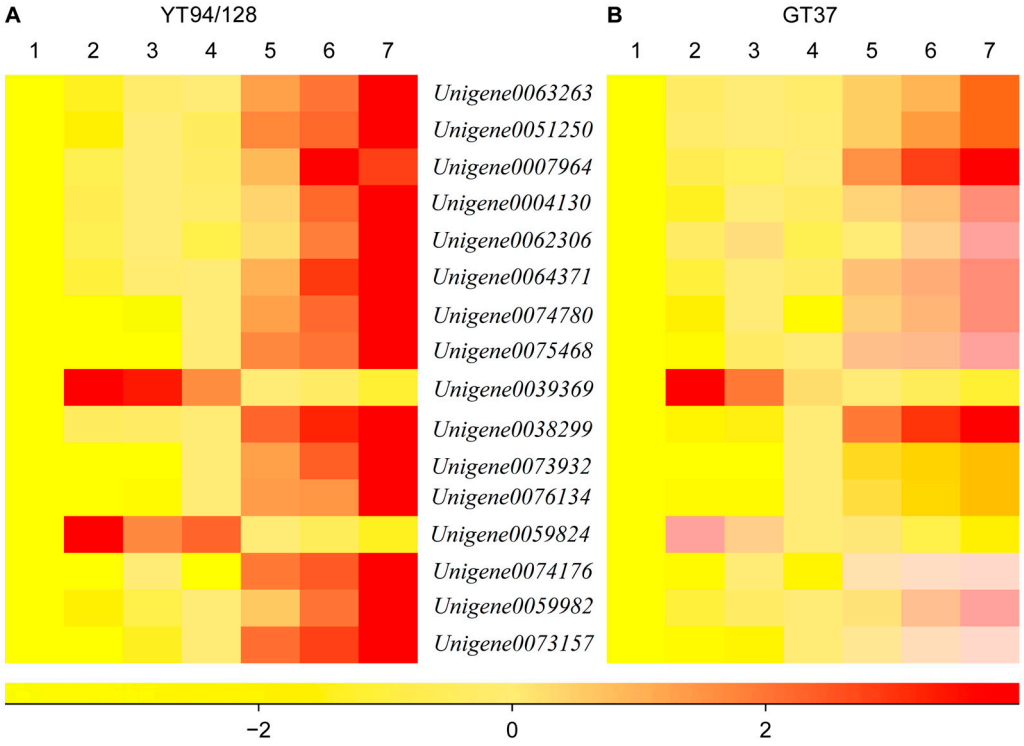

Figure 4. qRT-PCR results of selected genes for peroxisome biosynthesis. (**A**) YT94/128 (R-PI); (**B**) GT37 (S-PI). Numbers 1–7 indicate the number of days after inoculation with the pathogen. The yellower and redder colors indicate lower and higher gene expression abundances, respectively.

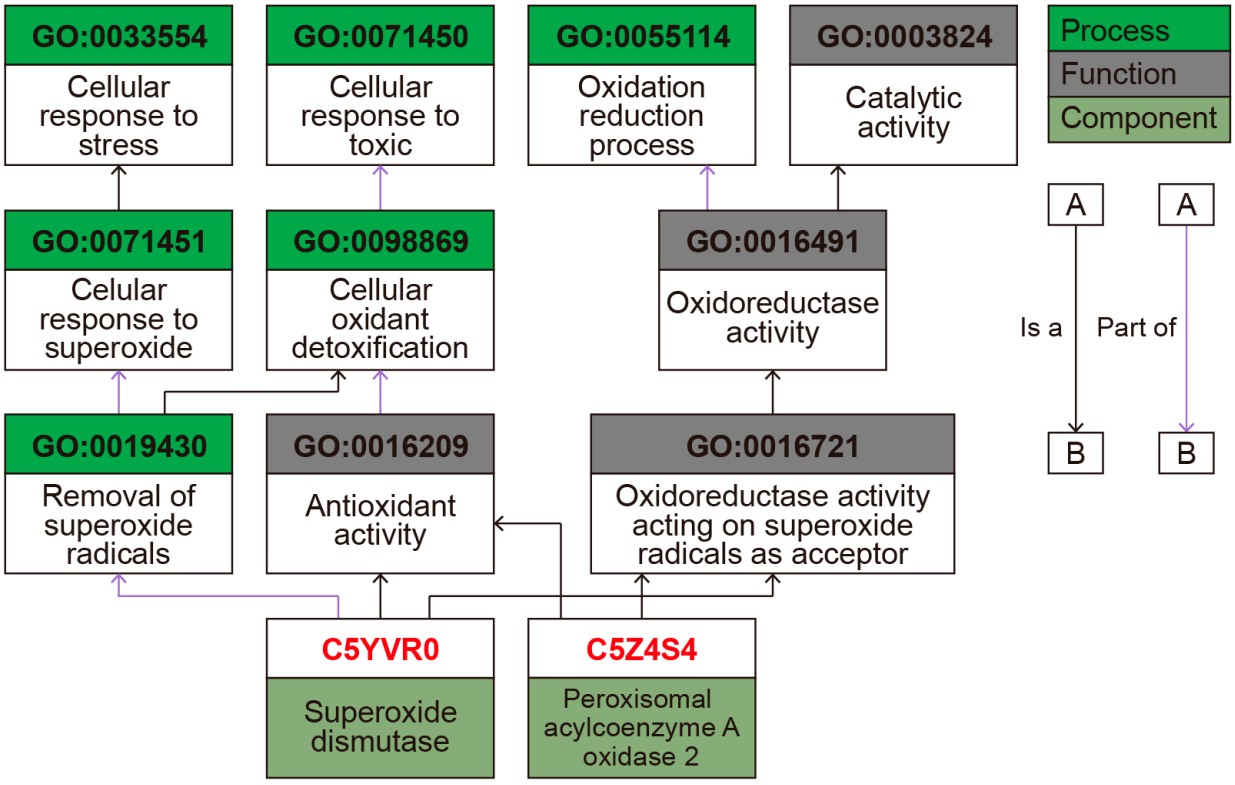

Figure 5. The metabolic processes related to C5YVR0 and C5Z4S4.

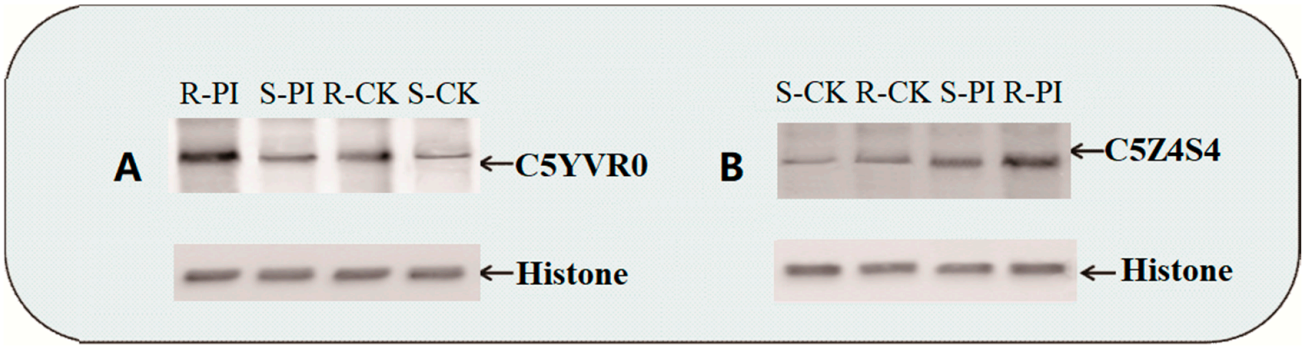

Figure 6. Protein expression trend with WB. (**A**) C5YVR0; (**B**) C5Z4S4.

4. Discussion

4.1. F. verticillioides Affects the Cytological Structure of Sugarcane and ROS Accumulation

Changes in plant cell membrane permeability and electrolyte leakage are the main physiological changes observed at the early infection stage. Changes in respiration, photosynthesis, nucleic acids and proteins, phenolic substances, water physiology, and other variables are also often observed [31]. Physical active-resistance factors limit pathogenic infection to local tissues [32]. *F. verticillioides* infection promotes wilting and toxin production in sugarcane, which damages the plasma membrane and induces morphological and structural changes at the subcellular, cellular, and tissue levels. Leaf epidermal cell wall calcification or silicification inhibits the invasion of pathogenic pectinase via plant cell division and the formation of protective tissues to replace the damaged cuticle, periderm, and/or other originally permeable barriers [33].

The sugarcane–*F. verticillioides* interaction causes the rapid necrosis of invaded cells and adjacent tissues, thus limiting *F. verticillioides* infection. Plant diseases are associated with ROS metabolism [34]. In addition, several key pathogenic interactions are associated with ROS production in the host. However, incompatibility interactions are significantly related to the enzymatic system [35]. ROS accumulation strengthens the cell wall, induces the synthesis of proteins that promote plant protection, and inhibits the growth of bacteria at the early pathogenic interaction stage. Substantial ROSs also induce hypersensitive reactions and cause cell apoptosis [34,36].

H_2O_2 is a product of membrane lipid peroxidation and an important indicator of oxidative stress. H_2O_2 accumulation was the highest in S-PI, followed by S-CK, R-PI, and R-CK, while no significant variations occurred among S-CK, R-PI, and R-CK at 7 d PI. However, wide and significant variations were observed among S-PI, S-CK, R-PI, and R-CK at both 14 d PI and 21 d PI (Figure 2A), indicating that several complex chemical reactions occur in sugarcane leaves after *F. verticillioides* infection. Some reactions, including changes in free amino acid compositions, physiological indicators associated with nitrogen metabolism, and differential expressions of antioxidant enzymes, are non-specific [37]. However, some reactions, including specific catalysis-induced responses and specific expressions of some resistance genes (gene-to-gene hypothesis), are specific [14,23]. Therefore, ROS-metabolism-related H_2O_2 activity induces the local resistance and systemic resistance of sugarcane to *F. verticillioides.* However, more studies are needed to determine the roles of ROSs in plant defense mechanisms and developmental processes.

4.2. Metabolic Mechanism of Peroxisome Resistance

ROSs increase the number of peroxisomes, suggesting that peroxisomes improve H_2O_2 detoxification in various cell parts, transmit signals, and promote the production of new proteins for defense purposes [30]. Fatty acids and the expressions of genes encoding the peroxisomal biogenesis factor (PEX) are essential for the proliferation of peroxisomes [38]. The expressions of *PMP34* and *MPV17* were significantly up-regulated in R-PI and S-PI, indicating that these genes are essential in maintaining H_2O_2 levels in sugarcane perox-

idases. The expressions of these genes were also associated with the expressions of the virulence genes of *F. verticillioides* based on the "gene-to-gene theory" proposed by Flor, which means that if there was a gene controlling disease resistance in the host, there would be a corresponding gene controlling disease pathogenicity in the agent. ROS-scavenging systems involved in defense in sugarcane were active under normal growth. However, the systems were not highly active under normal conditions; *F. verticillioides* altered this balance and led to significant increases in ROS accumulation in infected tissues.

SODs are a group of enzymes containing metal ions. SODs are mainly found in the cytoplasm, chloroplasts, mitochondria, and peroxidases in the form of Fe-SOD, Mn-SOD, and Cu/Zn-SOD. SOD activity is significantly altered after infection [39]. In this study, SOD activity significantly increased in R-PI and S-PI after *F. verticillioides* infection. However, SOD activity was higher in R than in S, which is inconsistent with the results of studies on interactions in other systems. Therefore, substantial ROS accumulation alters homeostasis and damages the cell membrane. However, the intrinsic ROS-scavenging system can quickly restore normal sugarcane growth. The differentially expressed *SOD* genes—*Unigene0033801*, *Unigene0076134*, and *Unigene0073932*—play key roles in disease resistance. There is, thus, a need to determine the specific functions of the DEGs to analyze the mechanisms underlying the resistance of sugarcane to PBD. The expression levels of some *SOD* genes were significantly lower in both R and S under the mock inoculation. However, their expression levels significantly increased following inoculation. Additional studies are needed to clarify these observations.

CAT is a marker enzyme in the peroxisome and plays key roles in H_2O_2 and water reduction reactions. CAT also mediates the responses of plants to various types of stress [40]. CAT activity was higher in S than in R. The expressions of CAT genes were the highest in S, indicating that the mechanisms of CAT accumulation vary among sugarcane plants with different genetic backgrounds; this suggests that CAT provides an effective physiological index for evaluating *F. verticillioides* resistance.

POD is an induced synthase, and its activity is associated with plant ROSs, lignin synthesis, and various oxidation reactions [41]. *F. verticillioides* infection significantly increased POD activity in sugarcane. Enzymatic activity was higher in R than in S, which is consistent with the results of studies on other crop–pathogen interaction systems. *PRDX5* (*Unigene0074176*) expression was significantly lower in normal sugarcane but considerably higher after inoculation, suggesting that *PRDX5* expression can be used as a PBD indicator. The expressions of genes involved in matrix protein import and receptor recycling, adenine nucleotide transport, peroxisome division, ROS metabolism, and processes related to peroxisomal membrane proteins were significantly up-regulated following the induction of POD, suggesting that POD biosynthesis enhances *F. verticillioides* resistance.

Analyses of metabolic processes, gene expressions, and enzymatic activities revealed the active oxygen metabolism pathway of *F. verticillioides*-infected sugarcane (Figure 7). Active oxygen species, including SOD, CAT, and POD, rapidly accumulated, and the characteristics of sugarcane during the mycelium's penetration of the cell wall were distinct following the accumulation of active oxygen species. Functional analysis and expression verification of related genes revealed six genes in sugarcane involved in the generation of H_2O_2 from HO_2, including *Unigene0073932*, *Unigene0076134*, and *Unigene0059824*. *Unigene0039369* and *Unigene0038299* were associated with O^- production from H_2O_2, and *Unigene0074176* was associated with the generation of $O_2^{\cdot-}$ and O_2. Decreases in SOD2A2 expression were consistent with changes in SOD levels, indicating that *Unigene0059824* affects the accumulation of SODs. Similarly, increases in *Unigene0038299* and *Unigene0074176* expressions were consistent with changes in CAT and POD levels, respectively, indicating that *Unigene0038299* and *Unigene0074176* expressions affect the accumulation of active oxygen radicals produced via both cellular metabolism and chemical reactions.

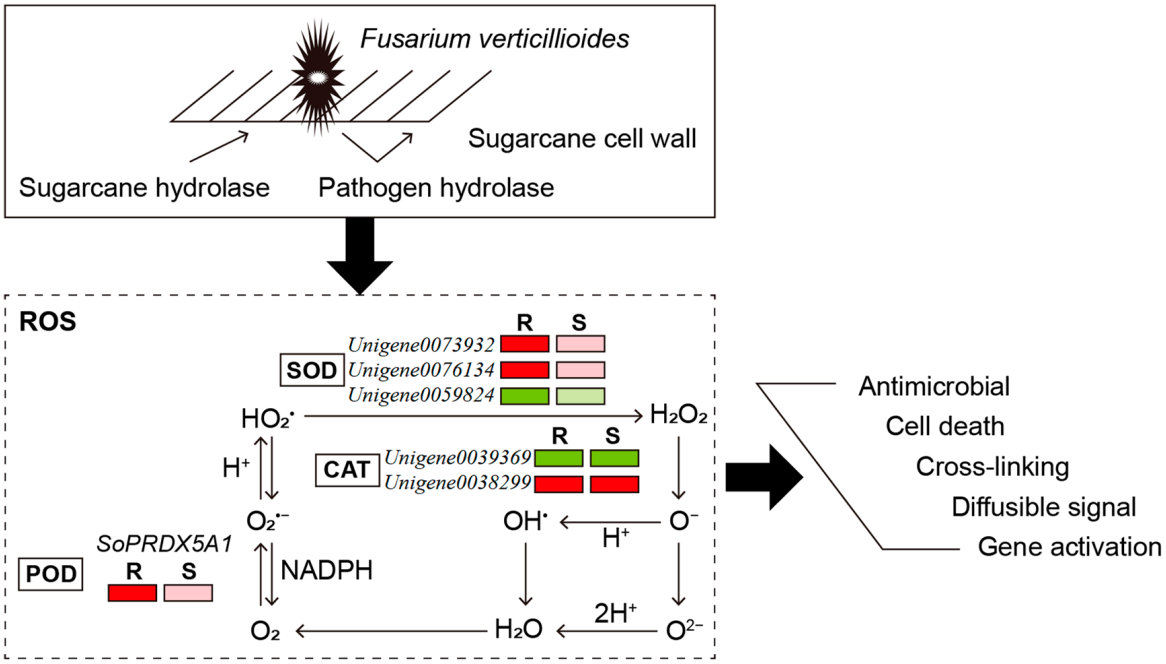

Figure 7. The active oxygen metabolism pathway involved in sugarcane's response to the pathogen causing PBD. Greener and redder colors indicate lower and higher gene expression abundances, respectively.

4.3. Potential Molecular Mechanisms Underlying the Response of Sugarcane to F. verticillioides

F. verticillioides is a neurotrophic fungal pathogen that has a major effect on sugarcane production. In this study, several sugarcane genes identified were involved in ROS production and redox regulation. Analyses of gene expressions revealed genes that were expressed constitutively and those that were expressed following exposure to pathogens. Protein verification results (C5YVR0 and C5Z4S4) also showed that peroxisomes are essential for normal sugarcane growth and metabolism. Organelles in the blade mediate the exchange of materials and transmit information; they, thus, play key roles in peroxisome-specific defense mechanisms in response to pathogenic infections [42].

Because of the complexity of the protein quality control methods involved in sugarcane–pathogen interactions, many specific mechanisms are still being explored. In conjunction with the existing topics of interest, we believe that, in the future, the following questions should be addressed: Are there proteins that can improve sugarcane's tolerance to pathogens? Are the effects discussed in this paper mainly because of sugarcane's improved ability to sequester pathogenic toxins in vacuoles (or other organelles) or something else? How can proteins recognize substrate proteins with different biological functions and three-dimensional structures and achieve efficient electron transport? Which chemicals serve as a selective energy source during metabolic stress to preserve the homeostasis and viability of sugarcane after PBD infection? Is/Are there one/multiple effector molecule(s) or marker(s) that explain(s) the resistant-gene-mediated ROS homeostasis regulation of sugarcane's self-repair mechanism? What substances are formed to reduce toxicity to plants? How does the antioxidant enzymatic system function in the process for effectively scavenging free radicals produced by pathogenic infections? In the future, we will also develop candidate disease resistance gene markers for identifying associations in the pathological system of the sugarcane–*F. verticillioides* interaction [43].

Therefore, ROS accumulation inhibits *F. verticillioides* infection, which blocks the secretion of *F. verticillioides* effectors. Our findings provide new insights into the immune mechanisms of sugarcane under pathogenic infection and will aid future studies aimed at clarifying the roles of ROSs in these resistance mechanisms. Our findings also shed new

light on the timing and production of ROSs during pathogenic infection, which allows for ROSs produced by plants and *F. verticillioides* to be distinguished.

5. Conclusions

The pathogen causing PBD affects ROS homeostasis in sugarcane leaves. After sugarcane infection, excess ROSs are not immediately eliminated, which results in rapid O^{2-} and H_2O_2 accumulation that reduces enzymatic activity and can even destroy the structures of several protective enzymes. Following pathogenic infection, the cell membrane's lipid peroxidation rate increases, and the membrane system is damaged, which causes cell death. The ROS scavenging system is a defense enzymatic system; *Unigene0073932*, *Unigene0076134*, *Unigene0059824*, *Unigene0039369*, *Unigene0038299*, *Unigene0074176*, and other peroxisome genes regulate the response of sugarcane to *F. verticillioides* to maintain ROS homeostasis. The fatty acid oxidation metabolism is also involved in this process. However, additional studies are needed to clarify the molecular mechanism underlying the metabolic and morphological changes in the peroxisomes of sugarcane following *F. verticillioides* infection.

Supplementary Materials: The following supporting information can be downloaded at https://www.mdpi.com/article/10.3390/agronomy14112640/s1, Table S1: The information of sugarcane peroxisome genes which indentified with RT-qPCR.

Author Contributions: Methodology, X.L. and Z.W.; investigation, X.L., C.Y., H.H., Y.L. and Z.W.; data curation, S.L., H.Y., L.L., Y.S. and Z.W.; writing—original draft preparation, X.L., C.Y. and Z.W.; writing—review and editing, Y.G.; funding acquisition, Y.G. and Z.W. All authors have read and agreed to the published version of the manuscript.

Funding: This research was funded by the National Natural Science Foundation of China (NNSFC 32260715), Central Government Guide's Local Funds for Science and Technology Development (GuiKe ZY21195033), Guangxi Major Science and Technology Project (GuiKe AA22117004), Guangxi Academy of Agricultural Sciences' Fund (Guinongke 2025YP065, GuiNongKeMeng 202403-1-5, GXAAS-WCJT 2024SC01, and GXGHTY2023SC01), Chinese Academy of Sciences' Foresight Strategic Science and Technology Project (XDA0450302), China Agriculture Research System of MOF and MARA–National Sugar Industry Technology System (CARS-17), and Province- and Ministry-Cosponsored Collaborative Innovation Center of the Canesugar Industry (No. 201812639).

Data Availability Statement: All the data supporting the findings of this study are available within the article and Supplementary Materials.

Conflicts of Interest: The authors declare no conflicts of interest.

References

1. Sydney, E.B.; Carvalho, J.C.; Letti, L.A.J.; Magalhaes, A.I.; Jr Karp, S.G.; Martinez-Burgos, W.J.; Candeo, E.S.; Rodrigues, C.; Vandenberghe, L.P.S.; Neto, C.J.D.; et al. Current developments and challenges of green technologies for the valorization of liquid, solid, and gaseous wastes from sugarcane ethanol production. *J. Hazard. Mater.* **2021**, *404*, 124059. [CrossRef]
2. Porika, J.; Yellagoni, S.; Reddy, E.; Gojuri, R.; Naguri, S. Evaluation of promising sugarcane clones in plant cane against natural infection of Pokkah Boeng Disease. *Curr. J. Appl. Sci. Technol.* **2020**, *39*, 129–134. [CrossRef]
3. Ali, A.; Khan, M.; Sharif, R.; Mujtaba, M.; Gao, S.J. Sugarcane Omics: An update on the current status of research and crop improvement. *Plants* **2019**, *8*, 344. [CrossRef] [PubMed]
4. Wang, Z.; Sun, H.; Guo, Q.; Xu, S.; Wang, J.; Lin, S.; Zhang, M. Artificial inoculation method of Pokkah Boeng disease of sugarcane and screening of resistant germplasm resources in subtropical China. *Sugar Tech* **2017**, *19*, 283–292. [CrossRef]
5. Sharma, D.D.K.; Kumar, A. Morphological, physiological and pathological variations among the isolates of *Fusarium moniliforme* Sheldon causing Pokkah Boeng of sugarcane. *Agrica* **2015**, *4*, 119–129. [CrossRef]
6. Lin, Z.; Wang, J.; Bao, Y.; Guo, Q.; Powell, C.A.; Xu, S.; Chen, B.; Zhang, M. Deciphering the transcriptomic response of *Fusarium verticillioides* in relation to nitrogen availability and the development of sugarcane Pokkah Boeng disease. *Sci. Rep.* **2016**, *6*, 29692. [CrossRef] [PubMed]
7. Wang, Z.; Liu, L.; Deng, Y.; Li, Y.; Zhang, G.; Lin, S.; He, T. Establishing a forecast mathematical model of sugarcane yield and brix reduction based on the extent of Pokkah Boeng disease. *Sugar Tech* **2017**, *19*, 656–661. [CrossRef]
8. Lorrai, R.; Ferrari, S. Host Cell Wall Damage during Pathogen Infection: Mechanisms of Perception and Role in Plant-Pathogen Interactions. *Plants* **2021**, *10*, 399. [CrossRef]

9. Waszczak, C.; Carmody, M.; Kangasjarvi, J. Reactive oxygen species in plant signaling. *Annu. Rev. Plant Biol.* **2018**, *69*, 209–236. [CrossRef]
10. Liu, Y.; Yu, Y.; Fei, S.; Chen, Y.; Xu, Y.; Zhu, Z.; He, Y. Overexpression of Sly-miR398b compromises disease resistance against *Botrytis cinerea* through regulating ROS homeostasis and JA-related defense genes in tomato. *Plants* **2023**, *12*, 2572. [CrossRef]
11. Piacentini, D.; Corpas, F.J.; D'Angeli, S.; Altamura, M.M.; Falasca, G. Cadmium and arsenic-induced-stress differentially modulates *Arabidopsis* root architecture, peroxisome distribution, enzymatic activities and their nitric oxide content. *Plant Physiol. Biochem.* **2020**, *148*, 312–323. [CrossRef] [PubMed]
12. Marti, L.; Savatin, D.V.; Gigli-Bisceglia, N.; de Turris, V.; Cervone, F.; De Lorenzo, G. The intracellular ROS accumulation in elicitor-induced immunity requires the multiple organelle-targeted *Arabidopsis* NPK1-related protein kinases. *Plant Cell Environ.* **2021**, *44*, 931–947. [CrossRef] [PubMed]
13. Moreau, S.; van Aubel, G.; Janky, R.; Van Cutsem, P. Chloroplast electron chain, ROS production, and redox homeostasis are modulated by COS-OGA elicitation in tomato (*Solanum lycopersicum*) leaves. *Front. Plant Sci.* **2020**, *11*, 597589. [CrossRef] [PubMed]
14. Pan, R.; Liu, J.; Wang, S.; Hu, J. Peroxisomes: Versatile organelles with diverse roles in plants. *New Phytol.* **2020**, *225*, 1410–1427. [CrossRef]
15. Pallavi, S.; Bhushan, J.A.; Shanker, D.R.; Mohammad, P. Reactive oxygen species, oxidative damage, and antioxidative defense mechanism in plants under stressful conditions. *J. Bot.* **2012**, *2012*, 217037. [CrossRef]
16. Rachowka, J.; Anielska-Mazur, A.; Bucholc, M.; Stephenson, K.; Kulik, A. SnRK2.10 kinase differentially modulates expression of hub WRKY transcription factors genes under salinity and oxidative stress in *Arabidopsis thaliana*. *Front. Plant Sci.* **2023**, *14*, 1135240. [CrossRef]
17. Ghozlan, M.H.; EL-Argawy, E.; Tokgöz, S.; Lakshman, D.K.; Mitra, A. Plant defense against necrotrophic pathogens. *Am. J. Plant Sci.* **2020**, *11*, 2122–2138. [CrossRef]
18. Peters, L.P.; Teixeira-Silva, N.S.; Bini, A.P.; Silva, M.M.L.; Moraes, N.; Crestana, G.S.; Creste, S.; Azevedo, R.A.; Carvalho, G.; Monteiro-Vitorello, C.B. Differential responses of genes and enzymes associated with ROS protective responses in the sugarcane smut fungus. *Fungal Biol.* **2020**, *124*, 1039–1051. [CrossRef]
19. Balamuralikrishnan, M.; Doraisamy, S.; Ganapathy, T.; Viswanathan, R. Effects of biotic and abiotic agents on sugarcane mosaic virus titre, oxidative enzymes and phenolics in sorghum bicolor. *Acta Phytopathol. Entomol. Hung.* **2005**, *40*, 9–22. [CrossRef]
20. Wang, Z.; Lin, S.; Liang, Q.; Li, Y.; Li, C.; Duan, W.; He, T. Effects of sugarcane canopy structure on Pokkah Boeng disease resistance. *J. China Agric. Univ.* **2017**, *22*, 40–46. [CrossRef]
21. Wang, Z.; Song, Q.; Shuai, L.; Reemon, H.; Mukesh, K.; Li, Y.; Liang, Q.; Zhang, G.; Zhang, M.; Zhou, F. Metabolic and proteomic analysis of nitrogen metabolism mechanisms involved in the sugarcane—*Fusarium verticillioides* interaction. *J. Plant Physiol.* **2020**, *251*, 153207. [CrossRef] [PubMed]
22. Gao, F.Y.; Li, L.; Wang, J.Y.; Wang, Y.L.; Sun, G.C. The functions of *PEX* genes in peroxisome biogenesis and pathogenicity in phytopathogenic fungi. *Hereditas* **2017**, *39*, 908–917. [CrossRef] [PubMed]
23. Akbar, S.; Wei, Y.; Yuan, Y.; Khan, M.T.; Qin, L.; Powell, C.A.; Chen, B.; Zhang, M. Gene expression profiling of reactive oxygen species (ROS) and antioxidant defense system following Sugarcane mosaic virus (SCMV) infection. *BMC Plant Biol.* **2020**, *20*, 532. [CrossRef] [PubMed]
24. Chen, J.; Li, Y.; Zeng, Z.; Zhao, X.; Zhang, Y.; Li, X.; Chen, J.; Shen, W. Silicon induces ROS scavengers, hormone signalling, antifungal metabolites, and silicon deposition against brown stripe disease in sugarcane. *Physiol. Plant.* **2024**, *176*, e14313. [CrossRef] [PubMed]
25. Wei, Y.S.; Zhao, J.Y.; Javed, T.; Ali, A.; Huang, M.T.; Fu, H.Y.; Zhang, H.L.; Gao, S.J. Insights into Reactive Oxygen Species Production Scavenging System Involved in Sugarcane Response to *Xanthomonas albilineans* Infection under Drought Stress. *Plants* **2024**, *13*, 862. [CrossRef]
26. Wang, Z.; Li, Y.; Li, C.; Song, X.; Lei, J.; Gao, Y.; Liang, Q. Comparative transcriptome profiling of resistant and susceptible sugarcane genotypes in response to the airborne pathogen *Fusarium verticillioides*. *Mol. Biol. Rep.* **2019**, *46*, 3777–3789. [CrossRef]
27. Livak, K.J.; Schmittgen, T.D. Analysis of relative gene expression data using real-time quantitative PCR and the 2(−Delta Delta C(T)) method. *Methods* **2001**, *25*, 402–408. [CrossRef]
28. St, L.; Wold, S. Analysis of variance (ANOVA). *Chemom. Intell. Lab. Syst.* **1989**, *6*, 259–272. [CrossRef]
29. Dunnett, C.W. A multiple comparison procedure for comparing several treatments with a control. *J. Am. Stat. Assoc.* **1955**, *50*, 1096–1121. [CrossRef]
30. Pan, R.; Reumann, S.; Lisik, P.; Tietz, S.; Olsen, L.J.; Hu, J. Proteome analysis of peroxisomes from dark-treated senescent *Arabidopsis* leaves. *J. Integr. Plant Biol.* **2018**, *60*, 1028–1050. [CrossRef]
31. Xu, Z.; Jiang, Y.; Zhou, G. Response and adaptation of photosynthesis, respiration, and antioxidant systems to elevated CO_2 with environmental stress in plants. *Front. Plant Sci.* **2015**, *6*, 701. [CrossRef] [PubMed]
32. Jones, J.D.; Dang, J.L. The plant immune system. *Nature* **2006**, *444*, 323–329. [CrossRef] [PubMed]
33. Lucas, W.J.; Groover, A.; Lichtenberger, R.; Furuta, K.; Yadav, S.R.; Helariutta, Y.; He, X.Q.; Fukuda, H.; Kang, J.; Brady, S.M.; et al. The plant vascular system: Evolution, development and functions. *J. Integr. Plant Biol.* **2013**, *55*, 294–388. [CrossRef] [PubMed]
34. Nanda, A.K.; Andrio, E.; Marino, D.; Pauly, N.; Dunand, C. Reactive oxygen species during plant-microorganism early interactions. *J. Integr. Plant Biol.* **2010**, *52*, 195–204. [CrossRef] [PubMed]

35. Barnard-Kubow, K.B.; McCoy, M.A.; Galloway, L.F. Biparental chloroplast inheritance leads to rescue from cytonuclear incompatibility. *New Phytol.* **2017**, *213*, 1466–1476. [CrossRef]
36. Rai, P.; Prasad, L.; Rai, P.K. Fungal effectors versus defense-related genes of *B. juncea* and the status of resistant transgenics against fungal pathogens. *Front. Plant Sci.* **2023**, *14*, 1139009. [CrossRef]
37. Wang, Z.; Li, Y.; Liang, Q.; Li, C.; Wei, J.; Liu, L.; Lin, S. Change of nitrogen metabolic indexs in different sugarcane varieties inoculated with Pokkah Boeng disease pathogen. *Plant Physiol. J.* **2017**, *53*, 1963–1970. [CrossRef]
38. Wright, Z.J.; Bartel, B. Peroxisomes form intralumenal vesicles with roles in fatty acid catabolism and protein compartmentalization in *Arabidopsis*. *Nat. Commun.* **2020**, *11*, 6221. [CrossRef] [PubMed]
39. Nordzieke, D.E.; Fernandes, T.R.; El Ghalid, M.; Turra, D.; Di Pietro, A. NADPH oxidase regulates chemotropic growth of the fungal pathogen *Fusarium oxysporum* towards the host plant. *New Phytol.* **2019**, *224*, 1600–1612. [CrossRef]
40. Valenzuela-Cota, D.F.; Buitimea-Cantua, G.V.; Plascencia-Jatomea, M.; Cinco-Moroyoqui, F.J.; Martinez-Higuera, A.A.; Rosas-Burgos, E.C. Inhibition of the antioxidant activity of catalase and superoxide dismutase from *Fusarium verticillioides* exposed to a *Jacquinia macrocarpa* antifungal fraction. *J. Environ. Sci. Health B* **2019**, *54*, 647–654. [CrossRef]
41. Liu, H.; Dong, S.; Li, M.; Gu, F.; Yang, G.; Guo, T.; Chen, Z.; Wang, J. The Class III peroxidase gene OsPrx30, transcriptionally modulated by the AT-hook protein OsATH1, mediates rice bacterial blight-induced ROS accumulation. *J. Integr. Plant Biol.* **2021**, *63*, 393–408. [CrossRef] [PubMed]
42. Reumann, S.; Babujee, L.; Ma, C.; Wienkoop, S.; Siemsen, T.; Antonicelli, G.E.; Rasche, N.; Luder, F.; Weckwerth, W.; Jahn, O. Proteome analysis of *Arabidopsis* leaf peroxisomes reveals novel targeting peptides, metabolic pathways, and defense mechanisms. *Plant Cell.* **2007**, *19*, 3170–3193. [CrossRef] [PubMed]
43. Poursakhi, S.R.; Asadi, H.A.G.; Nasr-Esfahani, M.; Abbasi, Z.; Hassanzadeh, H.K. Identification of novel associations of candidate marker genes with resistance to onion-fusarium basal rot interaction pathosystem. *Plant Gene* **2023**, *37*, 100440–100450. [CrossRef]